A New Reduction Route for the Synthesis of Nanoscale Metals and Metal Oxides with Ascorbic Acid at Low Temperature

M. Khorasani-Motlagh[*], M. Noroozifar and H. Shahroosvand

Department of Chemistry, University of Sistan & Baluchestan, P.O. Box 98155-147, Zahedan, Iran

Reduction of the transition metal complexes in aqueous solution has been investigated systematically by ascorbic acid as the reducing agent without the assistance of any surfactant. Nanoparticles of α-Mn_2O_3, Ag and Cu were synthesized directly through aqueous phase reduction at room temperature. Nanoscale metal oxides such as Co_3O_4, α-Fe_2O_3 and MoO_2 were obtained through ascorbic acid reduction in alkali medium at 40°C. All the products were characterized on their structure and micro-morphology by the X-ray diffraction (XRD) and atomic force microscopy (AFM). The particle size of metal and metal oxides was about 10-50 nm. The reaction details and features were described and discussed.

Keywords: Nanoparticle, Metal, Metal oxide, Reducing agent, Ascorbic acid

INTRODUCTION

Nanometer-scale materials with the size of 1–100 nm have been attracted considerable interest in recent years due to the departure of properties from bulk phases arising from quantum size effect. Over the past decade, a variety of techniques have been applied to fabricate nanostructures of a broad class of materials, ranging from ceramic dielectrics [1], semiconductors [2], metals [3], and metal oxides [4, 5]. Among these materials, transition metal oxides have been the subjects of scientific and technological attention owing to their interesting properties [6, 7].

Up to now, a large number of methods have been developed to synthesize metal oxides with specific particle sizes, such as microwave-induced hydrolysis [8-11], thermal decomposition of metal chelates [12,13], sol–gel process [14], thermal synthesis in non-aqueous medium [15], aerosol technique [16],

solid-state synthesis [17,18], pulsed laser ablation and condensation process [19] and solvothermal synthesis [20-22].

Recently a great deal of work has been done on using new reducing agents for preparing reduced metal oxides. These oxides are important for many applications such as catalysts, high energy density battery cathodes, magnetic material and so on [23-28]. Manthiaram *et al.* reported that alkali borohydrides can be used as the reducing agent to generate binary oxides MoO_2,Cr_2O_3 and some ternary oxides, $NaWO_3$ [29-33]. Hydroxylamine was used to produce transition metal oxides such as Fe_3O_4, VO_2 and MoO_2 at relatively low temperature by Goodenough *et al.* [34-35]. Transition nanoscale metal oxides were synthesized with hydrazine as reducing agent [36]. Recently, many efforts to fabricate different nanoparticles have been focused on using greener methods such as aqueous ascorbic acid as the reducing agent [37-42].

In the present work, we studied the reduction of transition metal complexes in aqueous solutions at low temperature with ascorbic acid as the reducing agent without the assistance of

---

*Corresponding author. E-mail: mkhorasani@chem.usb.ac.ir

any surfactant or stabilizer. Nanoscale metal oxides of α-Mn_2O_3, Co_3O_4, α-Fe_2O_3, MoO_2, nanoparticles of Ag and Cu were obtained.

EXPERIMENTAL

All reagents used in this study were obtained from Merck and Aldrich Chem. Co. X-ray powder diffraction (XRD) analysis was conducted on a Rigaku D/Max X-ray diffractometre with graphite monochromatic Cu Kα radiation (λ = 1.5418 Å) to verify the formation of products. Atomic force microscopy (AFM) image of the samples were collected on DME Scanning Probe Microscopy (SPM-Mahar Fan Abzar Co.) to determine size and phase of products.

The preparation of nanoscale metal oxides and metals were summarized in Scheme 1. A given amount of pure transition metal starting materials (see Table 1) were dissolved in distilled water and then more distilled water was added until its total volume reached up to 50 ml. After that, the ascorbic acid solution was slowly dripped into the solution under constant stirring until precipitates formed (step A, B in Scheme 1). If the precipitates were not formed, sodium hydroxide should be pre-added to adjust the pH value of the solution to the weak basic condition. The solution was heated up to 40˚C under stirring constant for 4 hours (step E in Scheme 1). The mole ratio between ascorbic acid and starting material is very important to obtain products; the exact amounts of ascorbic acid were reported in Table 1.

For the synthesis of nanoscale α-Mn_2O_3, Cu and Ag, the products have been obtained directly at room temperature with ascorbic acid as the reducing agent (Pathway I in Scheme 1).

For the synthesis of Co_3O_4, α-Fe_2O_3 and MoO_2, pH value of the solutions was increased to 9 with NaOH. The precipitates were formed when the solutions were heated up to 40˚C under stirring constant for 4 hours (Pathway II in Scheme 1).

Finally, the precipitates were allowed to settle overnight and collected by filtration and washing with water and ethanol (step C in Scheme 1). The precipitates were dried over night in vacuum at 80˚C for 5 h. and stored in desiccators (step D in Scheme 1).
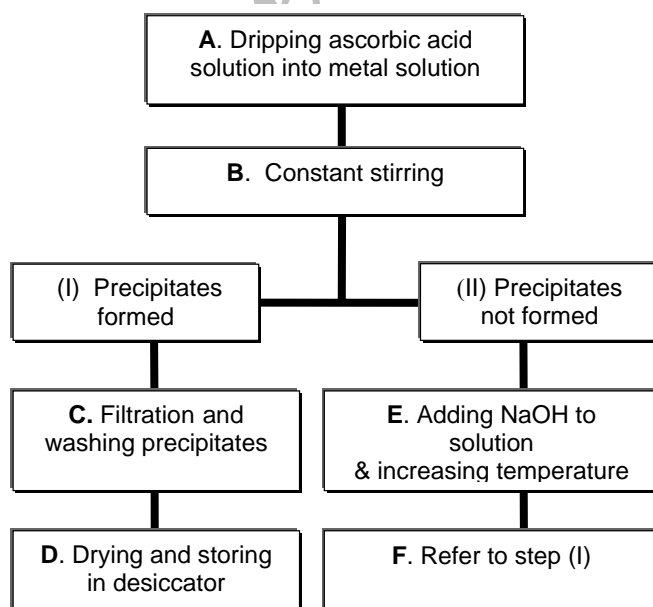
Scheme 1. The procedure of nanoparticles synthesis

RESULTS AND DISCUSSION

The optimum reaction conditions and the products obtained are listed in Table 1. The phase of samples has been studied by XRD. The morphology of the surface of all products has been studied by SPM with mode AFM.

It is interesting that the sample of manganese oxides was found directly by room temperature reduction without any surfactants. The XRD pattern as shown in Fig. 1a indicates the manganese oxides are crystalline in single-phase of cubic α-Mn_2O_3. No characteristic peaks of impurities can be detected. From the XRD data, the crystallite size (D_c) of α-Mn_2O_3 particles was calculated to be 15 nm, using Debye–Scherrer equation [43]:

$$D_c = \frac{K\lambda}{\beta \cos\theta}$$

where β is the breath of the observed diffraction line at its half-intensity maximum, K is the so-called shape factor, which usually takes a value about 0.9, and λ is the wavelength of the X-ray source used in XRD.

The AFM image of manganese oxides was reported in Fig. 2a. The sample has a mounded surface constituted of rounded grains grown on columnar pillars. The size of the crystals was found with an average diameter 16 nm. Also, the 3-D image of nanoproducts with area of 1.00 μm × 1.00 μm was reported in Fig. 2b. The phase image of α-Mn_2O_3 is shown in Fig. 2c. As seen in Fig. 2c, there is not any impurity with major product with potential range between -3.04 and -1.90 V.

The dripping speed of the ascorbic acid aqueous solution was a very important factor in preparing the α-Mn_2O_3. When ascorbic acid aqueous solution was dripped very slowly, the grains were formed with nano-size dimension and with increasing dripping speed; the grains with nano-size dimension were not formed. It determines the chemical reaction speed, which has an important effect on the growth of the nanometer-sized grains in aqueous solution.

For the synthesis of silver nanoparticles, after the short time of adding ascorbic acid into starting material, silver nanoparticle were formed on the surface of solution. As comparison with the work, Y.Liu *et al.* [37] using the ascorbic acid as the reducing agent with $AgNO_3$ as the starting material.

Table 1. The starting materials, reaction conditions and products obtained

Metal sources		Ascorbic acid		Conditions			Products	
Concentration (M)	Volume (ml)	Concentration (M)	Volume (ml)	pH	T (°C)	Size[a] (nm)	Size[b] (nm)	Final
$KMnO_4$ 0.2	50	4	15	4	25	16.3	15	α-Mn_2O_3
$AgNO_3$ 0.2	50	4	15	4	25	26.9	25	Ag
$CuSO_4$ 0.2	50	4	15	4	25	28.7	27	Cu
$Co(NO_3)_2$ 0.2	50	4	15	9	40	19.4	18	Co_3O_4
$Fe(NO_3)_2$ 0.2	50	4	15	9	40	22.5	20	α- Fe_2O_3
$MoCl_2$ 0.2	50	4	15	9	40	20.8	19	MoO_2

[a]: obtained from AFM images
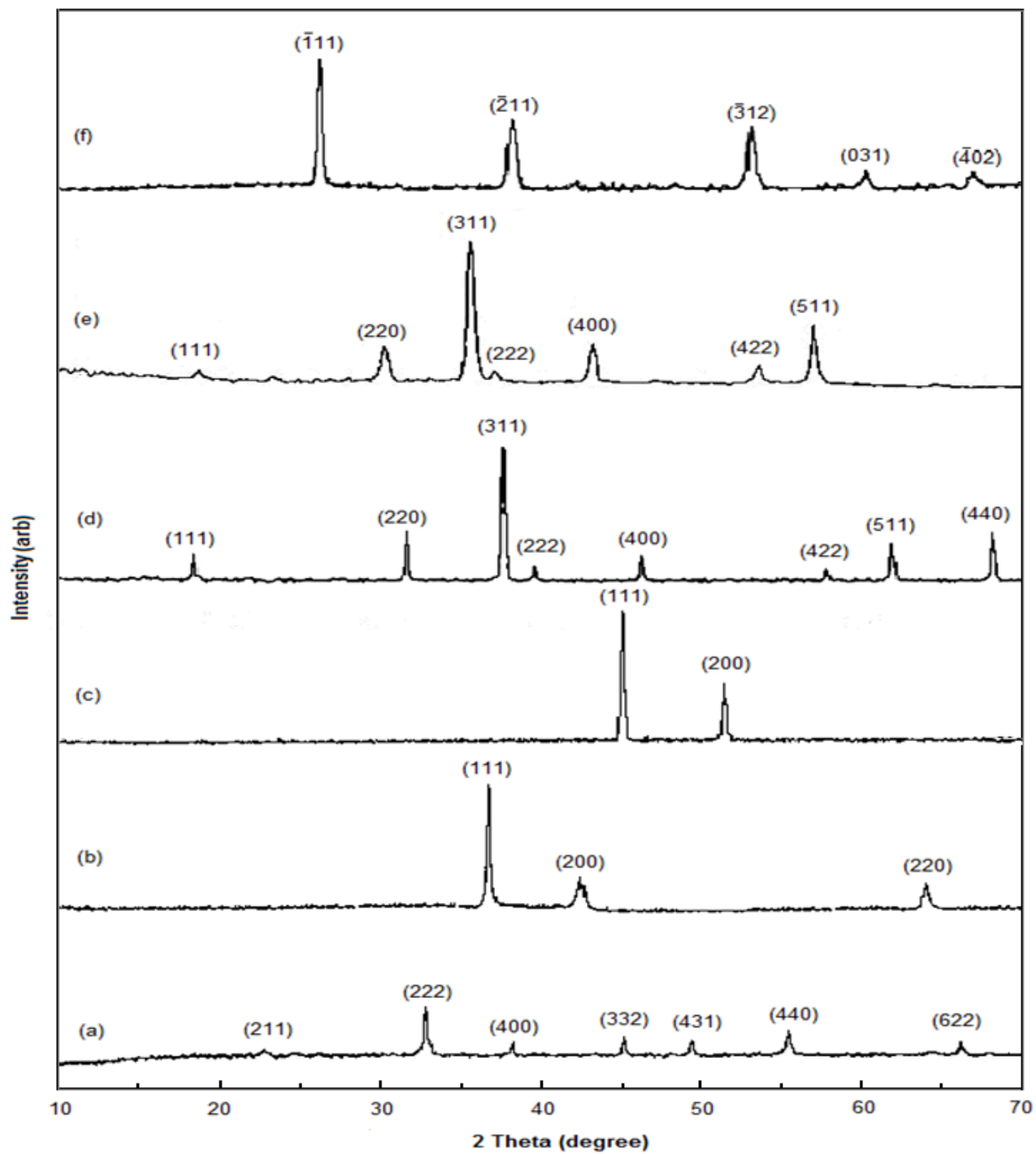
[b]: calculated from Debye–Scherer formula

Fig. 1. XRD patterns for the products of (a) α-Mn$_2$O$_3$, (b) Ag, (c) Cu, (d) Co$_3$O$_4$, (e) α-Fe$_2$O$_3$ and (f) MoO$_2$.

In their work, Ag nanowires were synthesized with using SDS/Ethanol/AgNO₃ system. In our suggested procedure, any surfactant was not used at low temperature. The XRD pattern of Ag nanoparticles was shown in Fig. 1b. This pattern indicates that Ag nanoparticles are crystalline in cubic structure. The crystallite size of silver calculated by the Debye-Scherrer equation were around 25 nm.

Fig. 2d shows the AFM topographic image of Ag nanoparticles. The sample has a mounded surface and the particle size is about 27 nm. The 3-D AFM image of Ag nanoproducts with Z-axis and the AFM phase image are reported in Fig. 2e, 2f respectively. From phase image, we can inform that there is not any effect of another particle with Ag nanoparticles. Here, the potential range was between -8.26 and -2.67 V.

The reduction of Cu^{2+} solution with ascorbic acid produced immediately golden colored Cu particles without the assistance of any surfactant. After addition of ascorbic acid into the solution, the solid Cu nanometer was formed. The XRD pattern for the prepared Cu nanoparticles was shown in Fig. 1c. All diffraction peaks of the sample can be readily indexed to the face center cubic phase of copper. No characteristic peaks of impurity phases such as CuO and starting material can be detected. The crystallite size of copper particles calculated by the Debye-Scherrer equation was around 27 nm.

The AFM topographic image of Cu nanoparticles (Fig. 2g) indicates the presence of islands with an average particle size 29 nm. The AFM image of the 3-D image Cu nanopruducts with Z-axis is shown in Fig. 2h. Fig. 2i of the AFM image is shown single-phase of Cu nanoparticles. The potential range was between -9.11 and -0.22 V.

It is found that the choice of starting materiel is important for preparation of Cu nanoparticles: if $CuCl_2$ is used instead of $CuSO_4$ as the starting material, keeping other experimental variables unchanged, the product is not pure Cu nanoparticles. In fact, the mixture of Cu and CuCl were formed. That is, because of the formation of undissolvable CuCl, which prohibits the further reduction of Cu (I) to Cu (0).

Various strategies have been developed for the synthesis of Co_3O_4 nanoparticles [15-22]. All of the methods need some special instruments, harsh conditions, and/or relatively high performance temperature. Recently, Co_3O_4 nanoparticles were synthesized by Zou *et al.* [44], using the ionic liquid-assisted in room temperature. The most important point is design a low temperature synthesis route which would allow the synthesis of Co_3O_4 at relatively low temperature. To our knowledge, this is the first report that the nanosiaze of Co_3O_4 can be directly synthesized through a simple redox method at low temperature without the assistance of any surfactant. The XRD pattern of Co_3O_4 nanoparticles was shown in Fig.1d. All diffraction peaks of the sample can be indexed to the cubic structure of Co_3O_4. The crystallite size of Co_3O_4 particles calculated by the Debye-Scherrer equation was around 18 nm.

The shape of Co_3O_4 products was further examined with AFM, as show in Fig. 2j. From the image, it can be seen remarkably that sample consisted of quantity of dispersive nanoparticle with the size about 19 nm. The 3-D image of Co_3O_4 nanoproducts with Z-axis is shown in Fig.2k. The phase image of Co_3O_4 is show pure phase as Fig.2l. This result was obtained through applied potential range between -8.81 and 2.36 V.

Some methods have been developed to synthesize iron oxide powders with specific particle sizes [45-48], comparing with mention methods, directly reduction synthesis has considerable advantages of a single step process at low temperature, composition and morphological control. The nanoparticles of α-Fe_2O_3 were obtained in alkali medium with dripping ascorbic acid into solution. The experimental results suggest that the nanoparticles were formed with increased in the pH value of the aqueous solution. The XRD pattern in Fig.1e indicates that resulting sample of single-phase α-Fe_2O_3. The particle size of the α-Fe_2O_3 powders was 20 nm, according to the Debye-Scherrer equation.

As shown in Fig.2m, the particle size of α-Fe_2O_3 nanoparticles is around 22 nm. The 3-D image of α-Fe_2O_3 nanoproducts with Z-axis is shown in Fig.2n. The phase image of α-Fe_2O_3 is shown in Fig.2o. From this image, at the potential range between -9.00 and -1.13 V, there is not any impurity with α-Fe_2O_3.
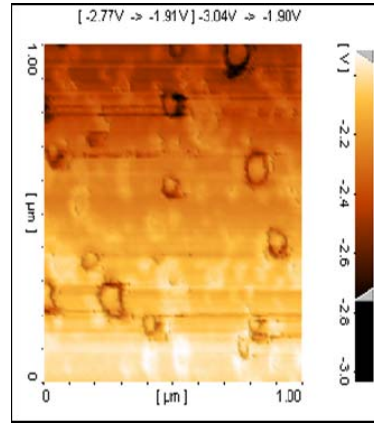
To date, MoO_2 nanocrystallites with different shapes have been fabricated under various conditions. Recently, Chen *et al.* [49] reported the synthesis of MoO_2 through a simple redox method with ethylene glycol as the reducing agent. According
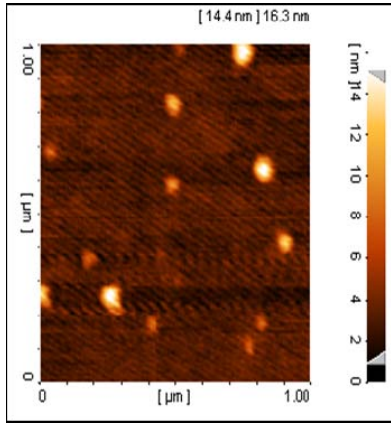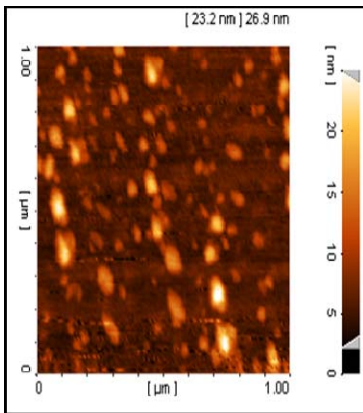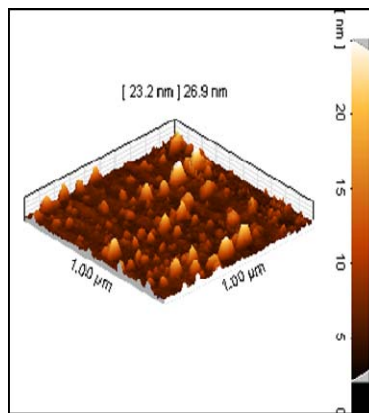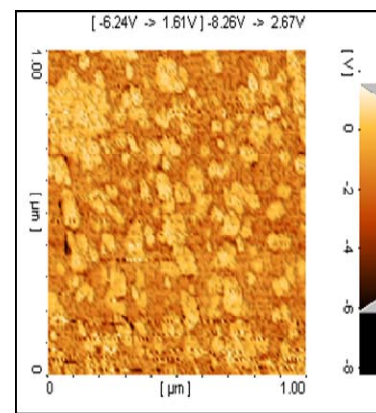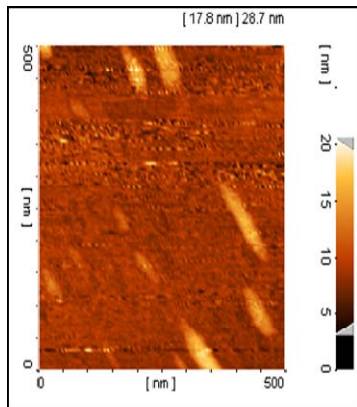
(a)
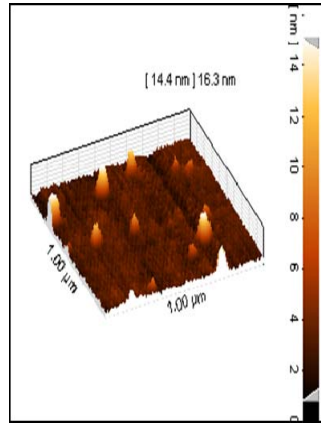
(b)

(c)

(d)

(e)

(f)

(g)
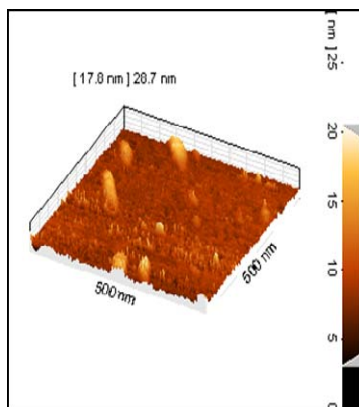
(h)
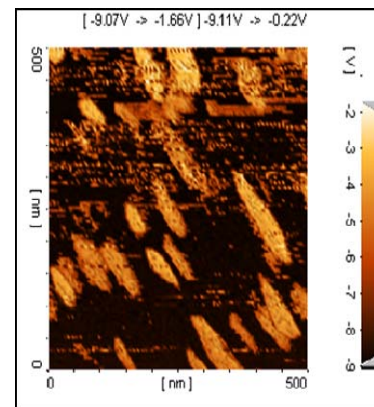
(i)

Fig. 2. AFM topographic images for the products of (a) α-Mn$_2$O$_3$, (d) Ag, (g) Cu, (j) Co$_3$O$_4$, (m) α-Fe$_2$O$_3$, (p) MoO$_2$; AFM 3-D images of (b) α-Mn$_2$O$_3$, (e) Ag, (h)Cu, (k) Co$_3$O$_4$, (n) α-Fe$_2$O$_3$, (q) MoO$_2$; AFM phase image for (c) α-Mn$_2$O$_3$, (f) Ag, (i) Cu, (l) Co$_3$O$_4$, (o) α-Fe$_2$O$_3$, (r) MoO$_2$.
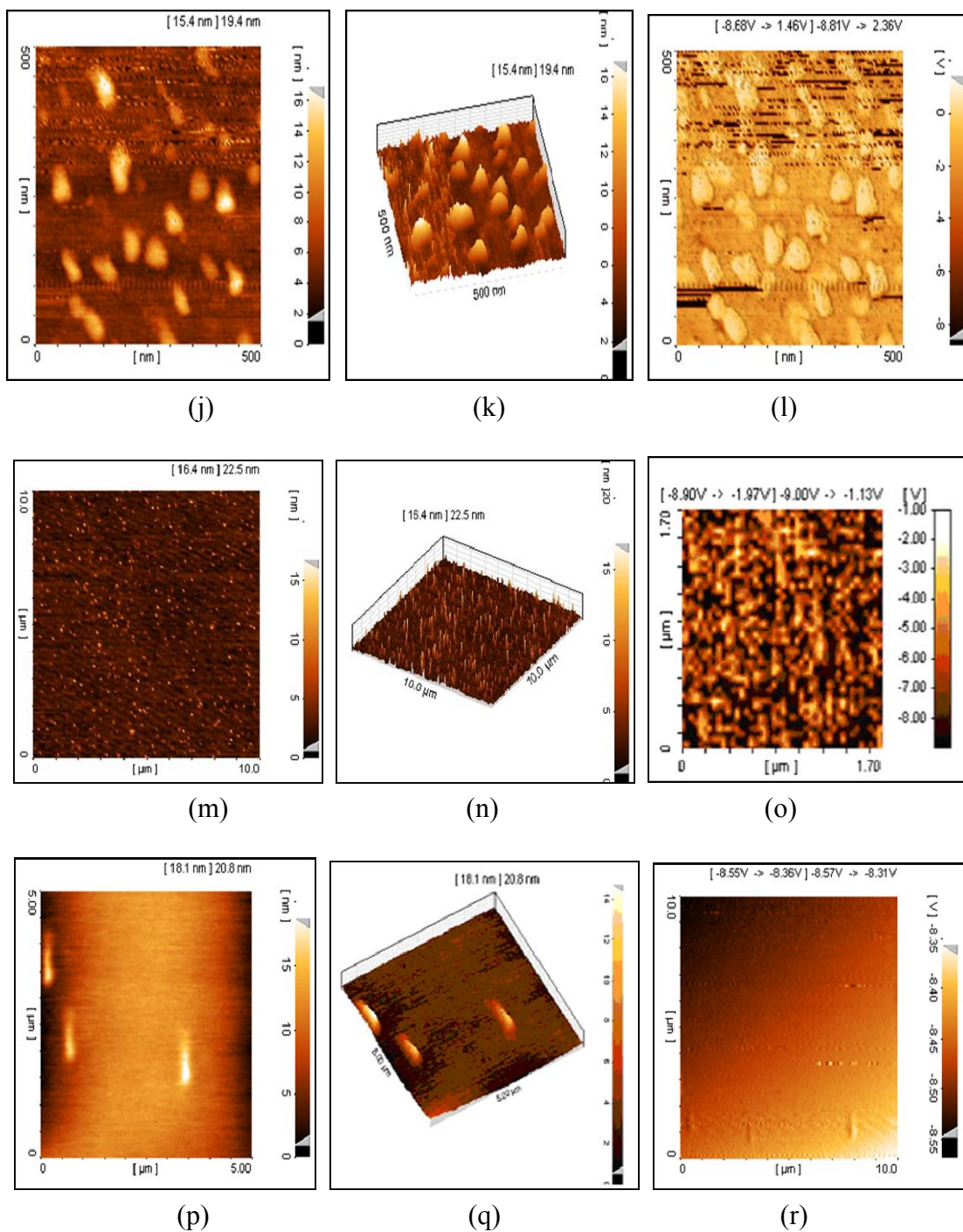
Table 2. Comparison of the results of different metal nanoparticles synthesized by reduction reaction using ascorbic acid as the reducing agent

Starting Material	Capping Agent	Temperature	pH	Product	Size(nm)	Ref.
$AgNO_3$	SDS	r.t.	4-5	Ag	8-10	37
$AgNO_3$	Citric acid	r.t.	4	Ag	20	38
$CuSO_4$	PVP	80 ºC	4-5	Cu	4	39
$HAuCl_4$	PVOH	r.t.	4-5	Au	50>	40
$Bi(NO_3)_3$	PVP	reflux / boiling point	10-11 / NaOH	Bi	50±10	41
$Fe(NO_3)_3$	-	r.t.	4-5	Fe	90>	42
$PdCl_2$	-	r.t.	4-5	Pd	50-80	42
Na_2PtCl_4	-	r.t.	4-5	Pt	70	42
$CuCl_2+HAuCl_4$	-	r.t.	4-5	Cu-Au	5-50	42
$Na_2PtCl_6+CuCl_2$	-	r.t.	4-5	Pt -Cu	50-60	42
$CuCl_2+PdCl_2$	-	r.t.	4-5	Cu-Pd	5-50	42
$Fe(NO_3)_3+ Na_2PtCl_6$	-	r.t	4-5	Fe-Pt	50>	42
$Fe(NO_3)_3+HAuCl_4$	-	r.t	4-5	Fe-Au	100>	42

PVP: poly(vinyl pyrrolidine), PVOH: poly(vinyl alcoh

ol), SDS: sodium dodecyl sulfate

to their results, the volume ratio of ethylene glycol as the reducing agent played a crucial role in the synthesis. In our work, MoO_2 nanoparticles were obtained in alkali medium at 40^oC. It is well shown that the heating effect drives the reaction to processed forward completely. The XRD pattern of MoO_2 nanoparticles is shown in Fig.1f. All diffraction peaks of the sample can be indexed to the monoclinic structure of MoO_2. According to the Debye-Scherrer equation, the particle size of MoO_2 nanoparticles was 19 nm.

Fig.2p is representative AFM topographic imaging of MoO_2 nanoparticles. It is seen that particle size is around 21 nm. AFM image of the 3-D image MoO_2 nanoproducts with Z-axis is shown in Fig.2q. AFM image in Fig.2r shows single-phase of MoO_2 as well. This result was found through using range potential between -8.57 and -8.31 V. It indicates that there is not any particle with obtained MoO_2 nanoparticles.

For comparison, the some results of different metal nanoparticles synthesized by reduction reaction method using ascorbic acid as the reducing agent have been shown in Table 2. In this work, we have synthesized some metal and metal oxide nanoparticles using ascorbic acid without the assistance of any capping agent or stabilizer. Also, as seen in Table 2, in some cases the crystallite size of metal and metal oxide nanoparticles synthesized by our purpose method is smaller than those observed, previously.

CONCLUSIONS

We have systematically studied the low temperature chemical reduction of some transition metal cations using ascorbic acid as the reductant in aqueous solution without any surfactant. Nanoscale metals Ag, Cu, and metal oxides

(α-Mn$_2$O$_3$, α-Fe$_2$O$_3$, Co$_3$O$_4$ and MoO$_2$) have been obtained with particle size about 10-50 nm. The structure and micro-morphology of the products were well characterized. Our results showed that the concentration and mole ratio of the reducing agent, dripping speed of reductant and the pH value of solution have a great effect to obtain products. The nanophase reduced transition metal oxides are technologically important for catalysts.

ACKNOWLEDGEMENTS

REFERENCES

[1] C. Liu, B. Zou, A.J. Ordinance, Z.J. Zhang, J. Am. Chem. Soc. 123 (2001) 4344.

[2] M.H. Huang, Y.Y. Wu, H. Feick, N. Tran, E. Weber, P.D. Yang, Adv. Mater. 13 (2001) 113.

[3] B. Kim, S.L. Tripp, A. Wei, J. Am. Chem. Soc. 123 (2001) 7955.

[4] B. Liu, H.C. Zeng, J. Am. Chem. Soc. 126 (2004) 8124.

[5] J.J. Teo, Y. Chang, H.C. Zeng, Langmuir 22 (2006) 7369.

[6] W.F.S. Spear, D.S. Tamhuser, Phys. Rev., B 7 (1973) 831.

[7] R.N. Singh, J.F. Koenig, G. Poillerat, P. Chartier, J. Electroanal. Chem. 314 (1991) 241.

[8] D. Dong, P. Hong, S. Dai, Mater. Res. Bull. 30 (1995) 531.

[9] X.B. Han, L. Huang, Z. Hui, J. Inorg. Mater. 14 (1999) 669.

[10] P. Rigneau, K. Bellon, I. Zahreddine, D. Stuerga, Eur. Phys. J. Appl. Phys. 7 (1999) 41.

[11] Q. Li, Y. Wei, Mater. Res. Bull. 33 (1998) 779.

[12] R.S. Sapieszko, E. Matijevic, J. Colloid Interface Sci. 74 (1980) 405.

[13] R. Zboril, M. Mashlan, K. Barcova, J. Walla, E. Ferrow, P. Martinec, Phys. Chem. Mater. 30 (2003) 620.

[14] W.T. Dong, C.S. Zhu, J. Mater. Chem. 12 (2002) 1676.

[15] P. Deb, A. Basumallick, P. Chatterjee, S.P. Sengupta, Scripta Mater. 45 (2001) 341.

[16] M.V. Cabanas, M. Vallet-Regi, J. Gonzalez-Calbet, J. Mater. Res. 8 (1993).

[17] C.X. Qiu, J.S. Jiang, Z.J. Zhao, X.L. Yang, J. Inorg. Mater. 16 (2001) 957.

[18] R. Zboril, M. Mashlan, K. Barcova, M. Vujtek, Hyperfine Interact. 139 (2002) 597.

[19] S.R. Shinde, A.G. Banpurkar, K.P. Adhi, A.V. Limaye, S.B. Ogale, S.K. Date, G. Marest, Mod. Phys. Lett. B 10 (1996) 1517.

[20] G.S. Li, R.L. Smith, H. Inomata, K. Arai, Mater. Res. Bull. 37 (2002) 949.

[21] H. Kominami, S. Onoue, K. Matsuo, Y. Kera, J. Am. Ceram. Soc. 82 (1999) 1937.

[22] D.H. Chen, X.L. Jiao, D.R. Chen, Mater. Res. Bull. 36 (2001) 1057.

[23] X. Wang, Y. Li, Chem. Commun. (2002) 764.

[24] R.N. Reddy, R.G. Reddy, J. Power Sources 124 (2003) 330.

[25] M. Toupin, T. Brousse, D. Belanger, Chem. Mater. 14 (2002) 3946.

[26] V. Subramanian, H.W. Zhu, R. Vajtai, P.M. Ajayan, B.Q. Wei, J. Phys. Chem. B 109 (2005) 20207.

[27] R.S. Sapieszko, E. Matijevic, J. Colloid Interface Sci. 74 (2) (1980) 405.

[28] D. Dong, P. Hong, S. Dai, Mater. Res. Bull. 30 (5) (1995) 531.

[29] C. Tsang, A. Dananjay, J. Kim, A. Manthiram, Inorg. Chem. 35 (1996) 50.

[30] C. Tsang, J. Kim, A. Manthiram, J. Mater. Chem. 8 (1998) 425.

[31] C. Tsang, J. Kim, A. Manthirm, J. Solid State Chem. 137 (1998) 28.

[32] C. Tsang, S.Y. Lai, A. Manthiram, Inorg. Chem. 36 (1997) 2206.

[33] Y.T. Zhu, A. Manthiram, J. Solid State Chem. 110 (1994) 187.

[34] V. Manivannan, R. Tichy, J.B. Goodenough, J. Solid State. Chem. 147 (1999) 269.

[35] V. Manivannan, J.B.Goodenough, Inorg. Chem. 37 (1998) 269.

[36] Z. Gui, R. Fan, W. Mo, X. Chen, L. Yang, Y. Hu, Materials Research Bulletin. 38 (2003) 169.

[37] Y. Liu, Y. Chu, L. Yang, D. Han, Z. Lu, Materials Research Bulletin.40 (2005) 1796.

[38] L. Hong, Q. Li, H. Lin, Y. Li, Mater. Res. Bull. 44 (2009) 1201.

[39] W. Yu, H. Xie, L. Chen, Y. Li, C. Zhang , Nanoscale Res Lett 4 (2009) 465.

[40] I. Yoon, A. M. Zimmerman, C. C. Tester, A. M. Didiccio, Y. Jiang, W. Chen, Chem. Mater. 21 (2009) 3924.

[41] R. Fu, S. Xu, Y. N. Lu, J. J. Zhu, Cryst. Growth Des. 5 (2005) 1379.

[42] M. N. Nadagouda, R. S. Varma, Cryst. Growth Des. 7 (2007) 2582.

[43] H. P. Klug, L. E. Alexander, X-ray Diffraction Procedures for Polycrystalline and Amorphous Material, second Ed., Wiley, New York, 1974.

[44] D. Zou, C. Xu, H. Luo, L. Wang, T. Ying, materials letters. 62 (2008) 1976.

[45] E. Mendelovici, R. Villalba, A. Sagarzu, Mater. Res. Bull. 17 (2) (1982) 241.

[46] M.V. Cabanas, M. Vallet-Regi, J. Gonzalez-Calbet, J. Mater. Res. 8 (1993) 2694.

[47] L. Markov, V. Blaskov, D. Klissurski, S. Nikolov, J. Mater. Sci. 25 (7) (1990) 3096.

[48] X. Li, E. Lin, C. Zhang, S. Li, J. Mater. Sci. Lett. 14 (19) (1995) 1335.

[49] X. Chen, Z. Zhang, X. Li, C. Shi, X. Li, Chemical Physics Letters. 418 (2006) 105.